Electronic Journal of Biotechnology 76 (2025) 1–11

Contents lists available at ScienceDirect

Electronic Journal of Biotechnology

journal homepage: www.elsevier.com/locate/ejbt

Research article

Metformin mitigates potassium bromate-induced liver grievance in rat through attenuating NF-kB and PI3K/Akt pathway ☆

Bo Ma [a,1], Sheng Zheng [b,1], Ning Xie [c], Juan Yang [d], Xueli Zeng [e], Pei Liu [e], Shunling Zhang [e], Ji Li [f,*]

[a] Department of General Surgery, The Second Affiliated Hospital of Xinjiang Medical University, Urumqi, Xinjiang, China
[b] Department of Gastroenterology, The Third People's Hospital of Yunnan Province, Kunming, Yunnan, China
[c] Department of Infectious Disease, The 908th Hospital of Chinese People's Liberation Army Joint Logistic Support Force, Nanchang, Jiangxi, China
[d] Department of Science and Education, The Third People's Hospital of Yunnan Province, Kunming, Yunnan, China
[e] Graduate School of Clinical Medicine, Dali University, Dali, Yunnan, China
[f] Department of Hepatobiliary Surgery, People's Hospital of He Chuan ChongQing Chongqing, China

GRAPHICAL ABSTRACT

Metformin mitigates potassium bromate induced liver grievance in rat through attenuating NF-kB and PI3K/Akt pathway.

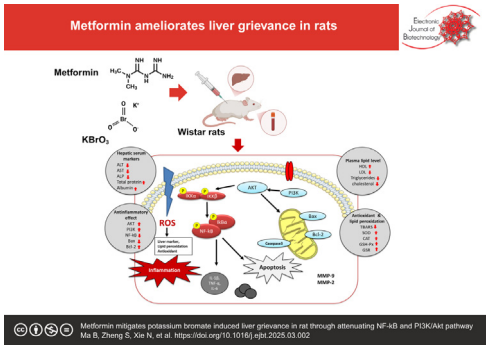

ARTICLE INFO

Article history:
Received 23 September 2024
Accepted 11 March 2025
Available online 8 May 2025

Keywords:
Antiinflammatory
Antioxidant activity
Hepatic cells
Hepatoprotectivity

ABSTRACT

Metformin (MET) is a dietary polyphenolic compound that exhibits anti-inflammatory and antioxidant properties. This study evaluated the protective effects of MET in both *in vitro* and *in vivo* models against potassium bromate ($KBrO_3$)-induced hepatotoxicity. Hepatic cells were exposed to $KBrO_3$ with or without metformin (20, 40, and 60 μM), and cell viability and Reactive Oxygen Species levels were assessed. *In vivo*, rats were divided into five groups: control, $KBrO_3$, and $KBrO_3$ with metformin (25, 50, and 100 mg/kg). Liver and blood samples were analyzed for histological changes, oxidative stress markers, lipid peroxidation, liver enzymes, and PI3K/Akt signaling.

Results: $KBrO_3$ exposure significantly decreased cell viability and increased ROS levels. Co-treatment with MET dose-dependently restored cell viability, with 60 μM MET achieving approximately 80% viability. Metformin also reduced ROS levels, with mean fluorescence intensity approaching control values at

☆ Audio abstract available in Supplementary material.

Peer review under responsibility of Pontificia Universidad Católica de Valparaíso

* Corresponding author.
E-mail address: liji2024318@outlook.com (J. Li).

[1] These authors contributed equally to this work.

https://doi.org/10.1016/j.ejbt.2025.03.002

Metformin
Oxidative stress
PI3K/Akt signaling
Potassium bromate
Properties
Rat

higher concentrations. In the *in vivo* study, $KBrO_3$ exposure elevated lipid peroxidation markers, depleted antioxidant enzyme activities, and triggered oxidative stress and inflammation. Metformin significantly alleviated histological liver damage, suppressed proinflammatory cytokines, enhanced antioxidant enzyme activities, and modulated the PI3K/Akt signaling pathway to promote cell survival and reduce oxidative injury.

Conclusions: Metformin effectively protects hepatic cells against $KBrO_3$-induced cytotoxicity by improving cell viability and reducing Reactive Oxygen Species levels. Metformin successfully mitigates $KBrO_3$-induced hepatic injury by reducing oxidative stress, modulating inflammatory pathways (NF-kB), and regulating the PI3K/Akt signaling cascade, offering molecular evidence of its hepatoprotective effects.

How to cite: Ma B, Zheng S, Xie N, et al. Metformin mitigates potassium bromate induced liver grievance in rat through attenuating NF-kB and PI3K/Akt pathway. Electron J Biotechnol 2025;76. https://doi.org/10.1016/j.ejbt.2025.03.002.

1. Introduction

Potassium bromate ($KBrO_3$) is widely utilized as an oxidizing substance, maturation agent, flavor enhancer, antiepileptic drug, and sedative in veterinary medicine, as well as a mono-therapy [1,2]. $KBrO_3$ has been used as a component of food for the last 90 years, primarily in the late material stage to provide dough pliability and durability during roasting while promoting bread rise [3]. Ahmad et al. [4] reported its use in fish paste products, cheese, and beer manufacturing. Oloyede and Sunmonu [5] noted its application in cold wave hair treatments, pharmaceuticals, and cosmetics. Additionally, $KBrO_3$ can arise as a byproduct during ozonization of bromide-containing water.

Free radicals produced as a result of $KBrO_3$ biotransformation oxidatively damage vital macromolecules, leading to kidney damage and malignancy in experimental rats [6]. $KBrO_3$ toxicity is dose-dependent and associated with significant histopathological changes, particularly in the liver, kidney, genome, and cytotoxicity. Oxidative stress and inflammation are primary drivers of $KBrO_3$'s hepatotoxic effects [7,8,9]. The primary organ responsible for metabolizing xenobiotics is the liver, which makes it susceptible to xenobiotic harm. Exposure to $KBrO_3$ induces hepatic injury [10] through oxidative stress, disrupting the balance between free radical generation and antioxidant defense, and damaging proteins, lipids, and nucleic acids [11].

According to Al-Mareed et al. [7] $KBrO_3$ has an impact on genotoxicity by inducing the creation of 8-OH-dG, which comprises one of the greatest numbers of prevalent DNA adducts. Additionally, the liver cells experienced oxidative stress, genotoxicity, and cytotoxic due to $KBrO_3$ [7]. Moreover, $KBrO_3$-triggered oxidative stress promotes high levels of proinflammatory factors such as TNF-α, IL-1b, NF-kB, exacerbating liver injury [12]. Nuclear factor erythroid 2–related factor 2 (Nrf2) is a crucial transcription factor that regulates cellular defense mechanisms against oxidative stress by modulating the expression of antioxidant and cytoprotective genes. Nrf2 activation has been shown to mitigate oxidative damage and inflammation, promoting cellular survival and resilience under stress conditions [13] Recent studies highlight Nrf2′s broader regulatory network and potential as a pharmacological target, including its crosstalk with the Keap1-Cul3 complex [14] and the role of dietary compounds in enhancing its activity against oxidative stress-induced pathologies [15]. MAPK and PI3K/Akt control Nrf2 and NF-kB, highlighting inflammation as a critical pathogenic mechanism in $KBrO_3$ liver toxicity and providing therapeutic targets.

Natural medicinal herbs have demonstrated hepatoprotective effects over recent decades. For instance, maltol inhibits apoptosis and inflammatory in CCl4-induced liver damage [16]; gentian extract reduces liver inflammation by blocking NF-kB translocation [17]; and green tea extract controls TLR 2/3 to reduce swelling [18]. Finding novel therapeutic molecules with anti-inflammatory and antioxidant qualities is thus necessary.

Metformin (MET), a widely used biguanide hypoglycemic drug for type 2 diabetes, has been in clinical use for over 50 years. MET improves glucose metabolism by reducing hepatic glucose production, primarily through gluconeogenesis inhibition [19]. Mechanisms include prevention of mitochondrial respiration, stimulating AMPK, reduction in hepatic energy state, and repression of cAMP signaling via phosphorylation of CREB-binding protein, which are some of the potential drivers of metformin's reduction of hepatic gluconeogenesis [20,21]. Recent studies highlight its potential for treating liver diseases and hepatic cancers [22]. MET also exhibits hepato- and nephro-protective effects by suppressing oxidative damage and inflammation [23,24,25].

Despite this, its efficacy against $KBrO_3$-induced hepatotoxicity remains underexplored. This study is the first to investigate MET's hepatoprotective properties against $KBrO_3$ toxicity, providing insights into its potential as a therapeutic agent against oxidative stress and inflammation-driven liver damage via modulation of NF-kB and PI3K/Akt signaling pathways.

2. Materials and methods

2.1. Chemicals and reagents

We purchased potassium bromate ($KBrO_3$) and metformin from Sigma-Aldrich in St. Louis, Missouri, in the United States. Malondialdehyde (MDA), superoxide dismutase (SOD), glutathione (GSH) assay kit, protein extraction kits, aspartate aminotransferase (AST) and alanine aminotransferase (ALT) assay kits, and hematoxylin-eosin staining (HE staining) kits were all purchased from Nanjing Jiancheng Bioengineering Co., Ltd. (Nanjing, China). The supplier of the enhanced chemiluminescence (ECL) kit was Shenyang Wanlei Biotechnology Co., Ltd. (Shenyang, China). Abcam (Cambridge, UK) provided the rabbit monoclonal antibody for anti-mouse inducible PI3K, Akt, IkBα, NF-kB, caspase-3, Bax, Bcl-2, and β-actin for Western blot. Goat anti-rabbit and goat anti-rat secondary antibodies were purchased from Santa Cruz, California, in the United States. In the present study, all additional compounds and solvents utilized in biochemical and histological investigations were employed at the molecular level.

2.2. Cell culture and maintenance

In this work, we investigated the hepatotoxicity generated by $KBrO_3$ using human hepato carcinoma cells (HepG2). The cell lines

were kept at 37°C and 5% CO_2 in a humidified environment after being grown in DMEM medium, which contains 10% FBS and 1% antibiotic solution. Cells were subsequently transmitted, incubated in a CO_2 incubator at 37°C, and utilized for tests once they reached above 80% proliferation.

2.3. Cell viability assay

To ascertain the nontoxic dosage of MET and $KBrO_3$ (12.5 μM) on HepG2 cells, the MTT test was used by Nivetha et al. [26]. The cells had equal distribution inside the well, with the last concentration being 100 μl of DMEM. Moreover, the plates containing the cells were placed in an incubator and left for a whole day. After the incubation period, the cells were treated with MET at different concentrations, ranging from 10 to 100 μM. A 24 h incubation period was followed by a $KBrO_3$ treatment of the cells after 1 h. To ascertain the vitality of the cells, an additional 100 μg of the MTT mixture was introduced to the wells and maintained for 4 h. Ultimately, 100 μl of DMSO was applied to the cells in order to loosen the violet formazan crystals. The plates were examined in Multimode at 570 nm.

2.4. Intracellular generation of ROS and mitochondrial transmembrane alter assay

The ROS generation experiment was conducted in accordance with previous directions [10]. Following a 30 min exposure to $KBrO_3$ control and a 12 h MET treatment, the HepG2 cells were washed with PBS and reconstituted in culture medium (serum-free) comprising 10 μM DCFHDA. Following that, ROS production was determined by flow cytometry. Using Rhodamine-123 (Rh-123) labeling and fluorescence intensity measurement, MET on $KBrO_3$ revealed that mitochondrial transmembrane change was assessed [10].

2.5. Animals and experimental plan

Wistar male rats were employed to assess the hepatotoxicity generated by $KBrO_3$ (6–8 weeks gestational; 20–25 g in bodyweight). The animal research procedures were approved by the People's Hospital of HeChuan ChongQing (Ethics approval number: 202402301) and carried out in accordance with the Guide for the Care and Use of Laboratory Animals (Ministry of Science and Technology of China, 2006). The rats were abode in a precisely free of contaminants temperature chamber with plenty of room to roam about. Each day, the animals were provided full animal care, including new bedding and a 12-hour light/dark cycle with unrestricted access to both nourishment and water, all while maintaining a room temperature. Following a week of acclimatization, rats were divided into five groups (n = 6) at randomly: Three distinct sets of rats were used: the normal group received oral saline only; the $KBrO_3$ group received $KBrO_3$ (100 mg/kg/body weight) orally [26]; and each of the three MET groups received $KBrO_3$ orally for a while to guarantee that the $KBrO_3$ components were fully absorbed; after that, they received MET at concentrations of 25, 50, and 100 mg/kg/b.wt., correspondingly. Six weeks of oral administration were spent. During the last treatment, all animals were given an intraperitoneal injection of 70 mg/kg pentobarbital to induce anesthesia after a 12 h fast. The eyes were promptly removed, and serum samples were separated by centrifugation at 3000 g for 10 min at 4°C, followed by 40 min at ambient temperature for biochemical evaluation. Following their dislocation to death, the anesthetized animals were promptly dissected, and liver samples were collected. The Second Affiliated Hospital of Xinjiang Medical University Experimental Animal Center received all of the dissected rat carcasses for centralized processing. A total of 10% formaldehyde was used to preserve liver pieces, and any leftover liver sections had been stored for later research at −80°C.

2.6. Activities of liver marker, lipid peroxidation and antioxidant enzymes

Serum ALT and AST, gamma-glutamyl transferase (GGT), albumin, total cholesterol (TC), triglycerides (TG), total lipid profile, total bilirubin (TB), and direct bilirubin (DB), concentrations were measured. Rat ELISA kits provided by Bioassay Technology Laboratory were used to analyze samples of plasma for tumor necrosis factor-α (TNF-α), interleukin-6 (IL-6), and interleukin-1 beta (IL-1β). Using the hydroxyproline identification kit (Sigma-Aldrich, St. Louis, MO, USA), the hepatic amount was measured in accordance with the company's procedure. Using commercial kits (lipid peroxidation), the intensities of thiobarbituric acid reactive substance (TBARS), conjugated dienes (CD), GSH, SOD, and MDA were measured. The producers' protocols were followed, and every procedure was completed.

2.7. Histological examination

Standard histopathology investigations were used to evaluate MET's protective effect against ethanol-mediated liver damage. Sections of the liver were sliced, embedded in paraffin, and stored in 10% formalin. Liver sections were kept corroded with hematoxylin and eosin staining for histological analysis. Through standardization, the degree of liver fibrosis was identified. Fibrotic area was evaluated using a light microscope (Olympus CH20i, Japan). Randomized design sampling is used to value histology.

2.8. Western blotting analysis

Liver tissues were broken down using phosphatase inhibitors and RIPA lysis buffer (Sangon Biotech Co., Ltd., Shanghai, China). Protein was separated into thirty micrograms using SDS-polyacrylamide, and after being treated for 2 h with bovine serum albumin (BSA), the protein was transferred to a PVDF membrane. The membranes were subjected to incubation for an entire night at 4°C using primary antibodies [PI3K, Akt, IkBα, NF-kB, caspase-3, Bax, Bcl-2]. Emitter Coupled Logic (ECL) substrate (Pierce Chemical Co., Rockford, IL, USA) was used to assess the intensities of proteins after they were incubated with comparable secondary antibodies (β-actin). The protein band was examined using Quantity One software, and Quantity One (Bio-Rad Laboratories, Hercules, USA) performed standard method analysis.

2.9. RT-PCR analysis

Liver sections were processed with a TL2020 crushing machine (DHS Life Science & Technology, Beijing, China). Using Trizol reagent (Invitrogen), and following the procedure of the manufacturer, whole RNA was removed from the liver sections. The expression intensities of inflammatory factors were examined by using real-time fluorescent quantitative rt-PCR. The reference gene used in this process was GAPDH. Using cycle threshold (Ct), the countenance intensities were examined and then using the 2^{-DDCt} method normalized to b-actin appearance. Results were obtained from triplicate experimentations. Table 1 shows the primers used in the PCR reactions.

2.10. Statistical investigation

The study's variables are all presented as mean ± SD, and ANOVA was used to establish statistical significance. A difference in significance was considered as $p < 0.05$ or 0.01, and a multiple

Table 1
List of primer sequences.

Genes	Primer forward	Primer reverse
IL-6	CCACTTCACAAGTCGGAGGCTTA	CCAGTTTGGTAGCATCCATCATTTC
IL-1b	TCCAGGATGAGGACATGAGCAC	GAACGTCACACACCAGCAGGTTA
TNF-a	TGGCAAATGTGAGAAACGAG	AAACCAGAACAGACCCAACG
β-actin	TCACTGCCACCCAGAAGAC	GAAGTCGCAGGAGACAACC

comparison test was performed using SPSS 24.0 software. GraphPad Prism 6.0.4 (GraphPad Software, Inc., San Diego, CA, USA) was the program used to represent the statistical graph.

3. Results

3.1. Met's impact on cell survival

The cytotoxic MTT test was employed to determine the non-toxic quantity of MET. Different amounts of MET and $KBrO_3$, alone and together, were treated with HepG2 cells. According to various findings, $KBrO_3$ (12.5 μM) causes toxicity to the liver cells of HepG2 cells. We also used the MTT test to measure the dose-dependent cytotoxicity of $KBrO_3$ in HepG2 cells. Reduced viability of 75%, 35%, and 22% was seen at increasing concentrations of MET (20, 40, and 60 μM) (Fig. 1a). Furthermore, we discovered that HepG2 cell growth was suppressed by $KBrO_3$ induction at a dose of 12.5 μM, whereas MET by itself and in conjunction with $KBrO_3$ demonstrated around 92% of cell viability in HepG2 cells (Fig. 1b). It has become evident that MET exhibited influenced by concentration hepatoprotective effects on HepG2 cells, attenuating the effects of $KBrO_3$.

3.2. MET reduced the formation of ROS in HepG2 cells stimulated with $KBrO_3$

The overabundance of reactive oxygen species (ROS) has been linked to oxidative stress or cell damage. HepG2 cells' overproduction of ROS was examined by DCFH-DA staining, as shown in Fig. 2, which also shows MET on $KBrO_3$. A significant degree of DCFH staining was identified using flow cytometry, which indicates enhanced ROS production in HepG2 cells treated with $KBrO_3$. When cells exposed to $KBrO_3$ show reduced fluorescence intensity, MET (100 μM) significantly quenches intracellular ROS. In HepG2 cells, MET treatment also inhibits the generation of ROS induced by $KBrO_3$. It was discovered in this study that 100 μM HepG2 cells were the significant protective dosage of MET.

3.3. MET reduces histological alterations in the liver

Histopathological tests were used to investigate MET on $KBrO_3$-induced liver injury. The normal group's liver lobules were found to be in good condition upon histopathological inspection using hematoxylin and eosin staining (Fig. 3), and the hepatocytes were organized radically. But the rats in the $KBrO_3$ group clearly had particulate and inflammatory-like cell infiltrations on their liver surface; this is particularly related to enlarged fatty vacuoles, serious liver injury, balloon disintegration of hepatocytes, and enlarged intercellular gaps. It is apparent that the $KBrO_3$ group had significant hepatocyte necrosis, nuclear constriction, and loss of activity. By contrast, the hepatocyte microstructure surrounding blood arteries was greatly alleviated by MET therapy. Overall, we discovered that, in comparison to other MET dosages like 25 and 50 mg/kg b.wt, MET at 100 mg/kg b.wt shows better protection against $KBrO_3$-induced hepatic damage. The MET groups did, however, exhibit better liver pathological alterations, such as reduced surface fibrosis, normal cell organization, and less nuclear degradation and necrosis.

3.4. MET reduces liver damage caused by $KBrO_3$

The health advantages of MET have been demonstrated by several recent research; however, its potential to protect against $KBrO_3$-induced hepatotoxicity remains to be investigated. *In vivo* evaluation of MET's hepatoprotective efficacy against $KBrO_3$-induced liver damage was conducted in this work. Acute mortality and aberrant behavior in animals were not seen when 100 mg/kg/-day was administered; hence, 100 mg/kg/day was employed in the further investigation, with Fig. 4 illustrating the experimental development. Body weight and liver index have been incorporated into the assessment markers used for the duration of the investigation. The untreated rat's mean weight remained comparatively stable at 39.11 ± 1.95 g during the entire study; however, the $KBrO_3$-exposed rat's typical body weight showed a decrease (31.85 ± 1.85 g) (Fig. 4a). In contrast, all rats treated with MET had an increase in weight (37.01 ± 1.23 g), and their liver index (4.30 ± 0.215 mg/g) (Fig. 4b) was substantially less compared to the animal of the $KBrO_3$-exposed category (5.361 ± 0.268 mg/g) ($p < 0.01$).

3.5. Effect of MET on the serum liver enzymes of experimental animals

The quantities of aminotransferases (ALT, AST) in serum were measured in order to evaluate the impact of MET on rat functioning of the liver. The rat liver was severely injured during the course of constant $KBrO_3$ inductive methods, as seen by the considerably raised ($p < 0.01$) levels of ALT (118.58 ± 1.23 U/L), AST (72.24 ± 1.27 U/L) (Figs. 4c,d). On the other hand, pre-treatment with MET at different 3 doses considerably reduced the rise in these markers ($p < 0.01$). While contrasted to further MET dosages, for instance, 25 and 50 mg/kg b.wt., we discovered that MET at 100 mg/kg b.wt., shown an impressive activity, suggesting that MET successfully deteriorated liver damage generated by $KBrO_3$.

Additionally, our research showed that, in comparison to control rats, $KBrO_3$ substantially ($p < 0.01$) raised liver dysfunction serum indicators, such as GGT, DB, and TB (Fig. 4e–g). Rats treated with MET showed a substantial ($p < 0.01$) decrease in their GGT, DB, and TB values when compared to the group treated with $KBrO_3$. This suggested that MET reduced $KBrO_3$-dependent liver damage by improving GGT, DB, and TB levels in a dose-dependent manner.

Furthermore, as compared to the normal control group, $KBrO_3$ markedly raised TC and TG (Fig. 4h,i). Conversely, compared to the $KBrO_3$ group, pre-treatment with MET substantially ($p < 0.01$) decreased $KBrO_3$-induced high TC and TG levels. 100 mg/kg MET shown remarkable action, successfully lowering $KBrO_3$-induced liver damage in comparison to lower dosages (25 and 50 mg/kg b.wt.). Similarly, we discovered that $KBrO_3$ induction led to a substantial ($p < 0.01$) drop in albumin levels when compared to the control group. In contrast to the $KBrO_3$ group, the MET therapy at the three distinct dosages rose considerably ($p < 0.01$). 100 mg/kg b.wt showed remarkable action in comparison to lower MET dosages (25 and 50 mg/kg b.wt.) (Fig. 4j).

3.6. MET treatment ameliorates $KBrO_3$-exposed oxidative stress injury and lipid peroxidation measurement

While comparing the $KBrO_3$-exposed rat hepatocytes to the control rats' liver, there was a noticeable increase in the lipid peroxide by-products TBARS and CD (Figs. 5a, b). Conversely, lipid peroxides, TBARS, and CD content of rat liver tissues subjected to $KBrO_3$ were significantly decreased by MET administration at three different dosages (25, 50, and 100 mg/kg bw). The amount of oxidative stress markers in the liver has been determined in order

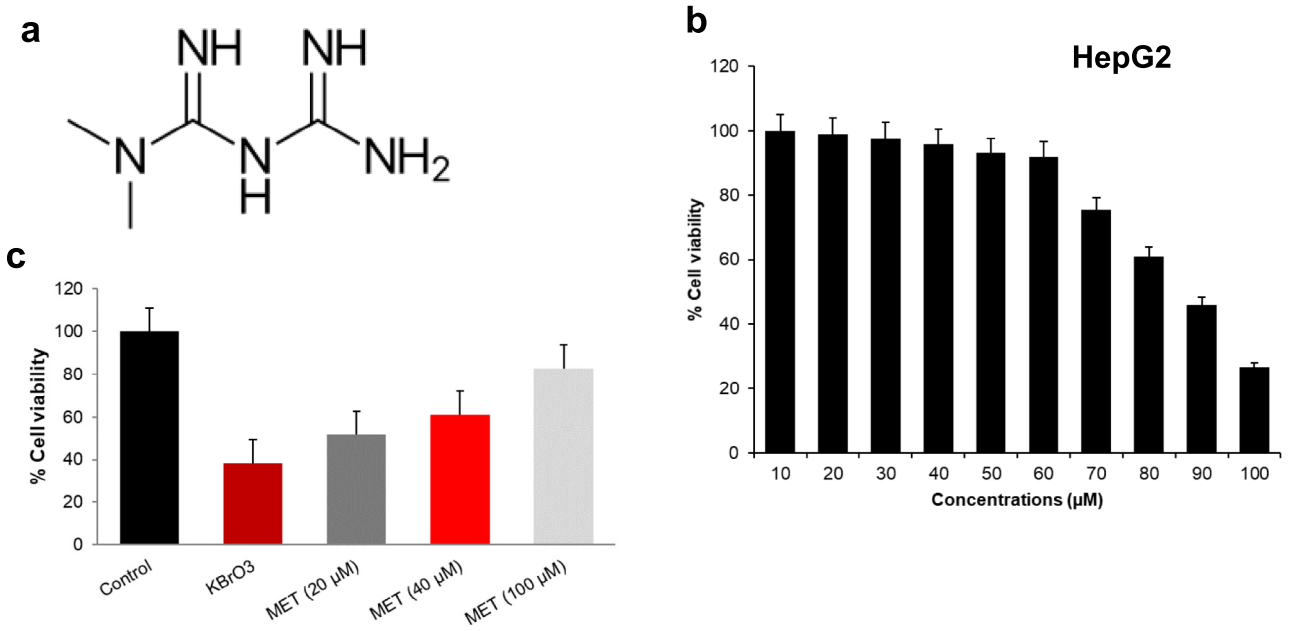

Fig. 1. MET suppresses $KBrO_3$ from inducing cytotoxicity in human HepG2 cells. (a) The chemical structure of metformin. (b) MET and associated non-toxic HepG2 levels without $KBrO_3$ therapy. (c). The MTT test measures the impact of MET on $KBrO_3$-exposed cytotoxicity in HepG2 cells. The outcomes across each group's six experiments are shown as means ± SD.

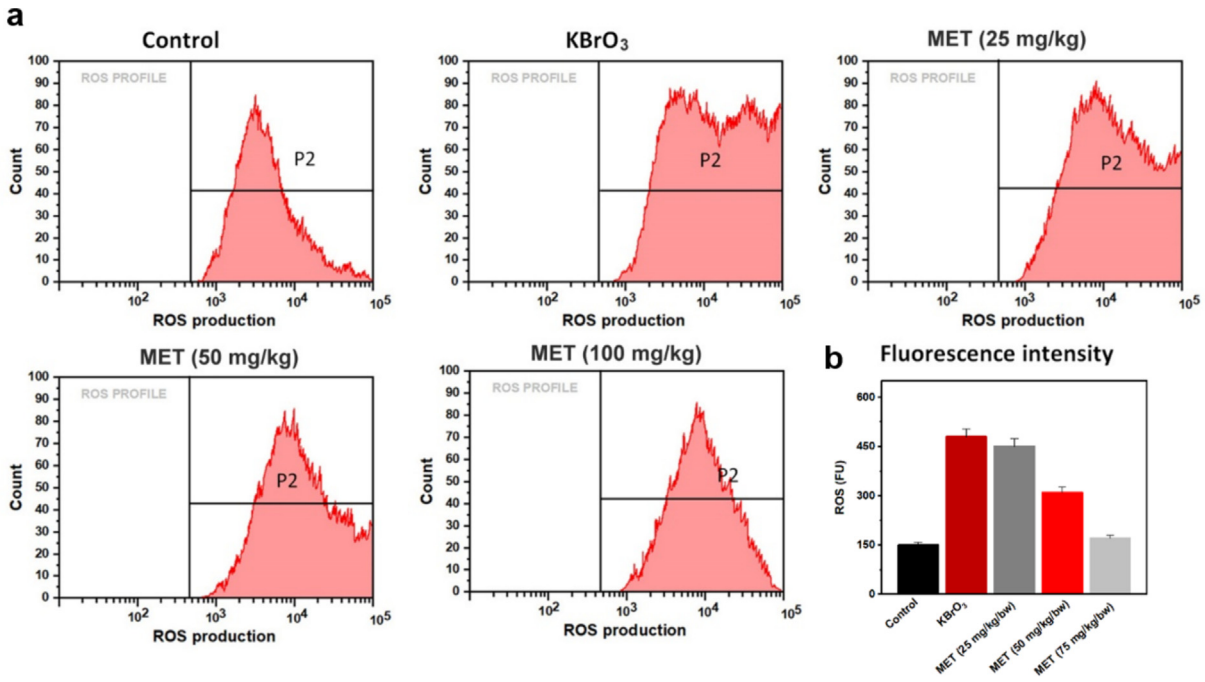

Fig. 2. Impact of MET on ROS in HepG2 cells exposed to $KBrO_3$ via DCFH-DA and flow cytometry. (a) Using a flow cytometer, the degree of intracellular ROS buildup was quantified and dyed with DCFH-DA. (b) Quantitative evaluation of intracellular ROS levels. Values are not sharing a common marking differ significantly at $p < 0.05$ (Duncan's multiple-range test).

to confirm if oxidative stress had a role in the $KBrO_3$-exposed hepatotoxicity in rats. In the $KBrO_3$ group, the levels of GSH (4.98 ± 0. 249 mol/g), SOD (23.41 ± 1.17 U/mg) were considerably lower ($p < 0.01$) in the liver contrasted to the control group. On the other hand, the quantities of MDA and LDH (5.98 ± 0.29 nmol/ mg) were substantially higher in the $KBrO_3$-exposed liver damage (Fig. 5c–f). In contrast to the $KBrO_3$-exposeded category, the amount of MDA in the liver decreased (3.11 ± 0.15 nmol/ mg) with MET therapy, while GSH (7.1 ± 0.355 l mol/g) and SOD (50.67 ± 2.53 U/mg) were substantially raised. From these results, we confirm that MET not only reduces oxidative stress but also boosts the antioxidant defense mechanism.

3.7. MET treatment restrains $KBrO_3$-induced liver inflammatory pathway in rat liver tissues

The NF-kB pathway is frequently exploited as a key signaling component in the inflammatory response, and inflammatory

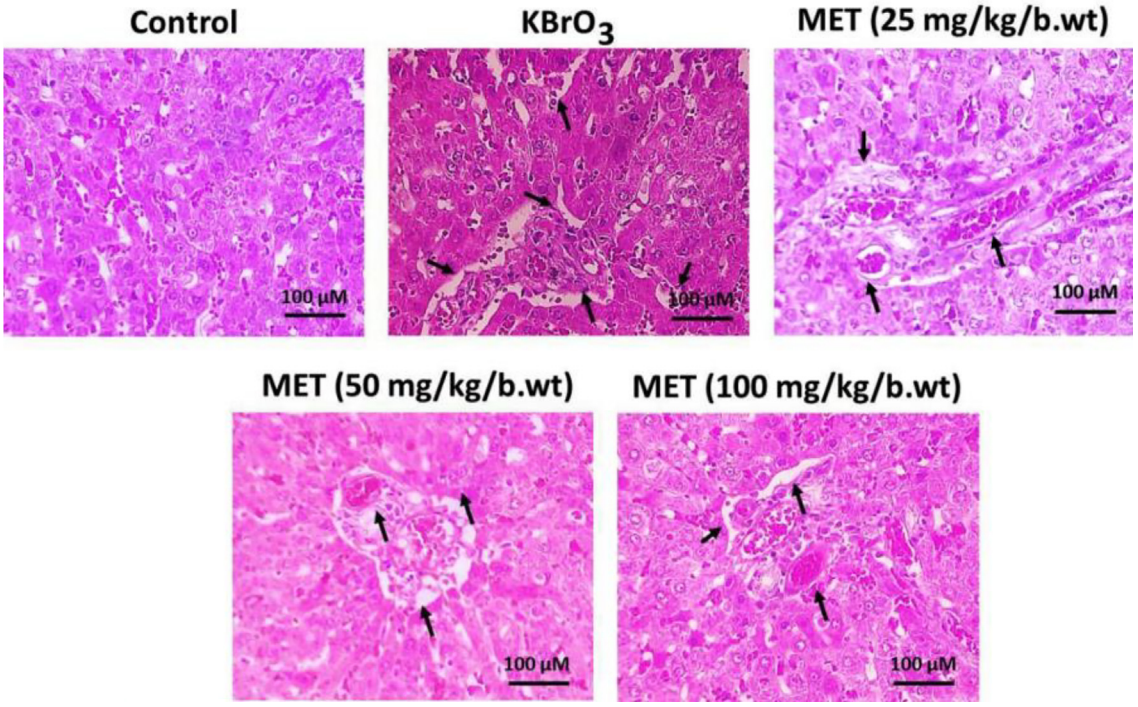

Fig. 3. Histopathological tests were used to investigate MET on $KBrO_3$-induced liver injury. The control group's liver lobules were found to be in good condition upon histopathological inspection using hematoxylin and eosin staining. It is apparent that the $KBrO_3$ group had significant hepatocyte necrosis, nuclear constriction, and loss of activity. By contrast, the hepatocyte microstructure surrounding blood arteries was greatly alleviated by MET therapy. Other MET dosages like 25 and 50, and 100 mg/kg b.wt, show better protection against $KBrO_3$-induced hepatic damage.

factors frequently exhibit aberrant behavior in the $KBrO_3$-induced liver damage model. Interestingly, Fig. 6a–c shows that the MET treatment dramatically decreased the expression of NF-kB and IkB α proteins ($p < 0.01$). MET's ability to suppress additional inflammatory mediators (TNF-α, IL-1β, and IL-6) in liver tissue subjected to $KBrO_3$ was investigated concurrently using rt-PCR (Fig. 6d–f). The findings demonstrated that the mRNA expression of provocative mediators across all dose categories was substantially reduced after MET therapy contrasted to the $KBrO_3$ group, alongside the enhancement associated with MET 100 mg/kg being especially noticeable (Fig. 6).

3.8. MET suppressed the apoptosis in $KBrO_3$-induced hepatocytes

An essential function of the Caspase protein family is to mediate apoptosis. One important regulatory component involved in several apoptotic regulatory pathways is caspase-3. Consequently, we employed western blot analysis to detect the positive expression of caspase-3 protein in order to ascertain if MET reduces $KBrO_3$-induced hepatocyte death. The $KBrO_3$ group of rats showed considerably higher expression of caspase-3 ($p < 0.01$) than the normal group, while the normal group showed almost no aberrant expression of the caspase-3 protein component (Fig. 7). On the other hand, the expression of caspase-3 was substantially suppressed by MET continuous pre-treatment ($p < 0.05$). Furthermore, $KBrO_3$ treatment induces apoptosis in rat liver tissue as demonstrated in Fig. 7 by noticing an elevated level of Bax and a reduction in Bcl-2 expression in comparison with standard control rat liver tissue. MET treatments, as opposed to $KBrO_3$-treated animals alone, prevented $KBrO_3$-mediated Bax, caspase-3 reduction, and elevated Bcl-2 levels in rat hepatic tissue apoptosis (Fig. 7a–d).

In order to investigate the molecular process by which MET prevents $KBrO_3$-induced hepatocyte cell death, Western blotting was used to investigate the PI3K/AKT signaling pathway (Fig. 8). The findings showed that p-PI3K and p-AKT protein levels declined following continuous $KBrO_3$ induction, but both of these were improved following MET treatment ($p < 0.01$) (Fig. 8a). We found that MET at 100 mg/kg bw is apparently a remarkable performance in contrast with different MET doses, including 25 and 50 mg/kg bw (Figs. 8b,c).

4. Discussion

Potassium bromate ($KBrO_3$) is widely recognized for its hazardous effects, notably as a neutralizer in domestic freezing shock hair kits and as a bread enhancer [5]. Its use has been implicated in numerous cases of unintentional child poisoning, leading many nations to ban its application due to its toxicity [3]. In the current investigation, we explored the biochemical alterations induced by $KBrO_3$ exposure and evaluated the hepatoprotective impact of MET in mitigating these toxic effects. A popular therapeutic drug, metformin, has several advantages and acts via various signaling pathways [27]. Anti-hyperglycemia is metformin's greatest quality. Metformin has been shown in cellular and animal experiments to limit the synthesis of glucose in the liver by inhibiting the regulation of gluconeogenic genes in either an independent or AMPK-dependent route [28]. In addition, metformin lowers blood sugar levels via altering the gut flora, improving glucose transport and absorption, or decreasing lactate consumption for gluconeogenesis. Metformin has been shown in accumulated clinical studies to offer benefits for a variety of malignancies. Furthermore, experiments have confirmed the valuable property of metformin on age-related illnesses, obesity, cardiovascular disease, liver disorders, and renal diseases, ultimately lowering the risk of mortality [29]. Thus, we assessed MET's hepatoprotective impact and process on the toxic effects of KBrO3 exposure to the liver in rats.

Introduction of $KBrO_3$ starts a number of pathways of cell signaling and causes oxidative stress. We demonstrated the

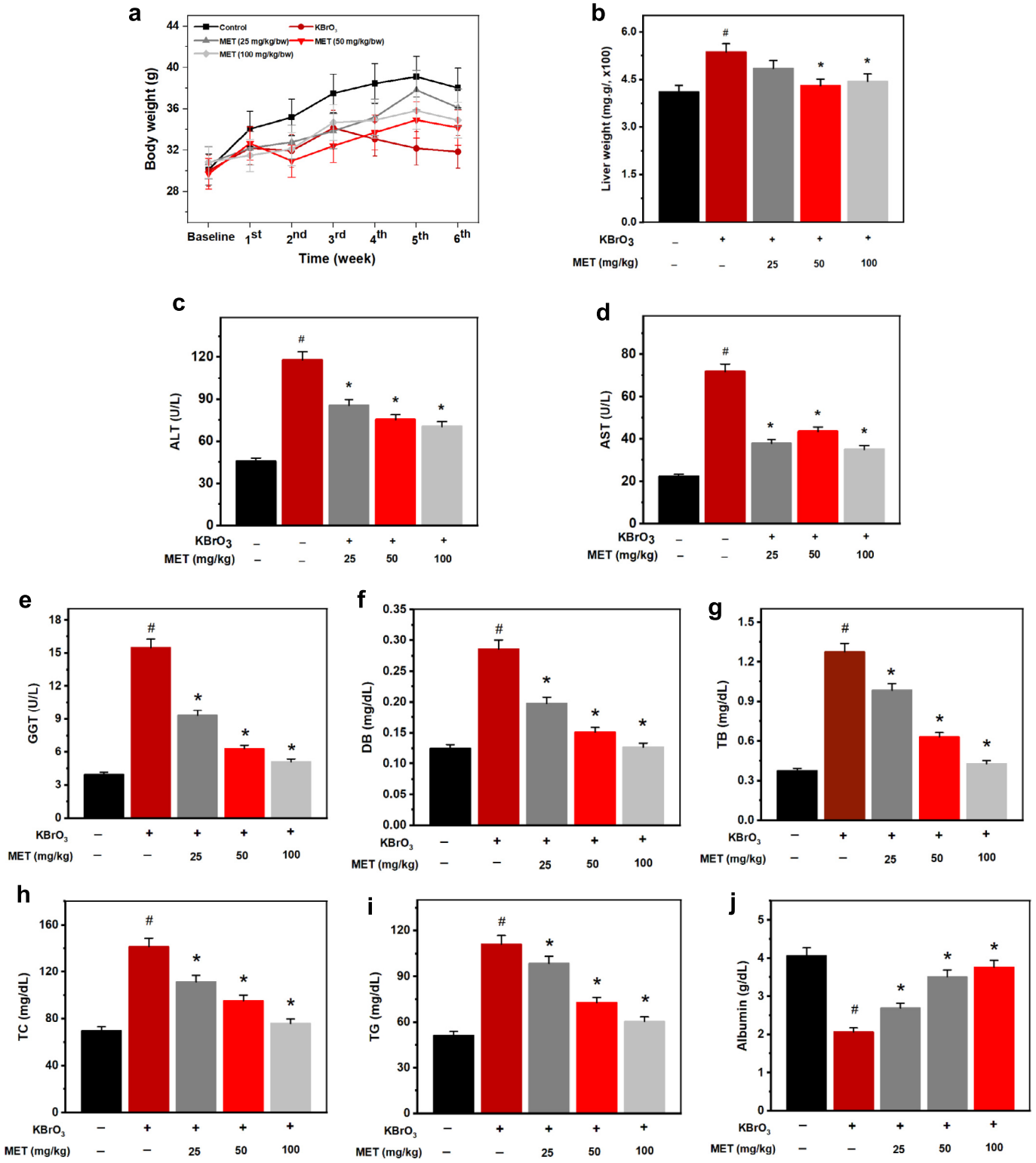

Fig. 4. (a) Effect of MET on body weight change among different experimental groups; (b) Liver weight, serum ALT (c); and AST (d) levels among different experimental groups. Serum indicators, such as GGT, DB, and TB (e,f,g), TC and TG (h,i), albumin levels (j). Data are mean ± SD. n = 10 per group. #p < 0.01 vs. Normal group; *p < 0.01 vs. $KBrO_3$ group.

hepatoprotective impact of MET on HepG2 cells caused by $KBrO_3$. MET protects against oxidative stress in various tissues and exhibits a range of biological functions [30]. Metformin's therapeutic potential in counteracting these effects was evident in our study. MET demonstrated a significant hepatoprotective effect against $KBrO_3$-induced cytotoxicity in HepG2 cells. At concentrations of 20, 40, and 60 μM combined with $KBrO_3$ (12.5 μM), MET effectively reduced ROS production, stabilized mitochondrial membrane potential, and mitigated oxidative damage. This finding underscores MET's capacity to attenuate $KBrO_3$-induced hepatotoxicity,

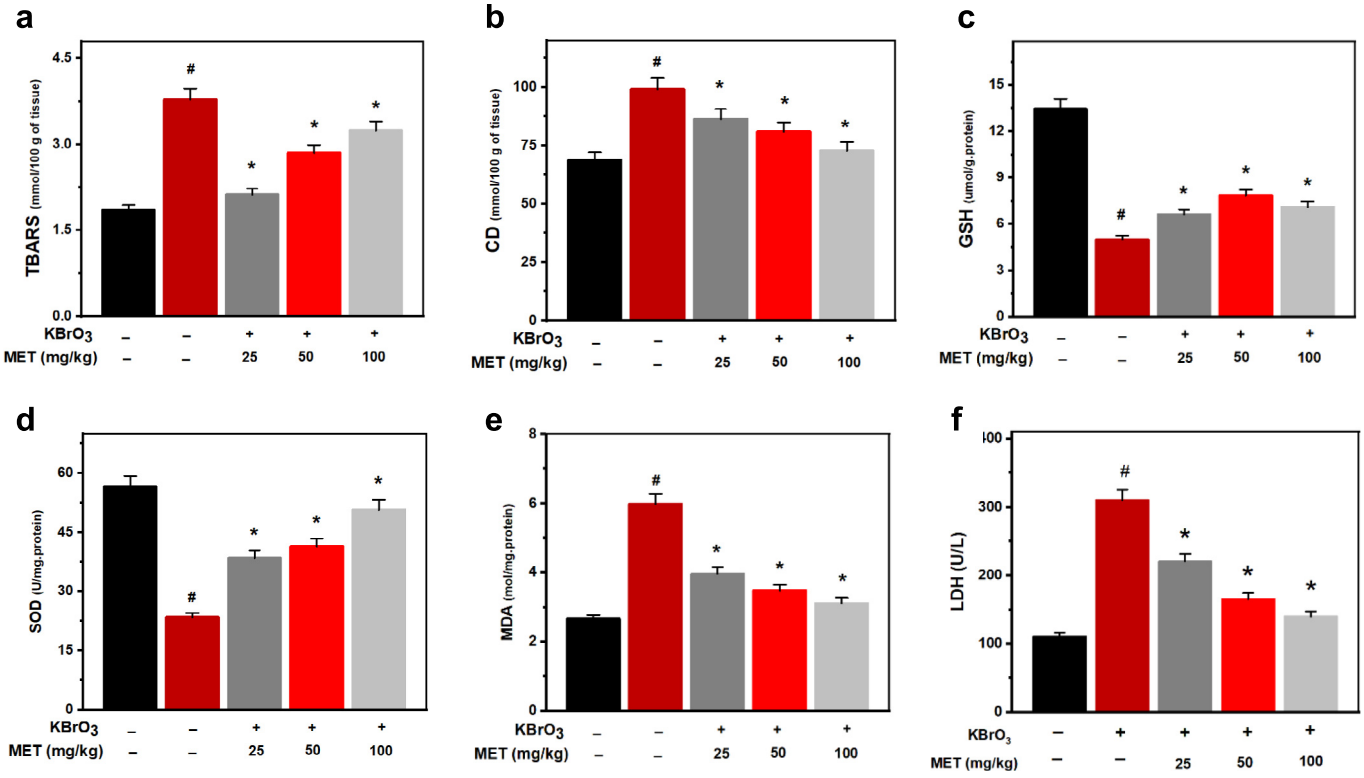

Fig. 5. Metformin reverses the effects of $KBrO_3$-induced increased lipid peroxidation TBARS (a) and CD (b). Impact of metformin on hepatic GSH (c), SOD (d), MDA (e), LDH (f) in rats induced with $KBrO_3$. Data are mean ± SD. n = 10 per group. #p < 0.01 vs. Normal group; *p < 0.01 vs. $KBrO_3$ group.

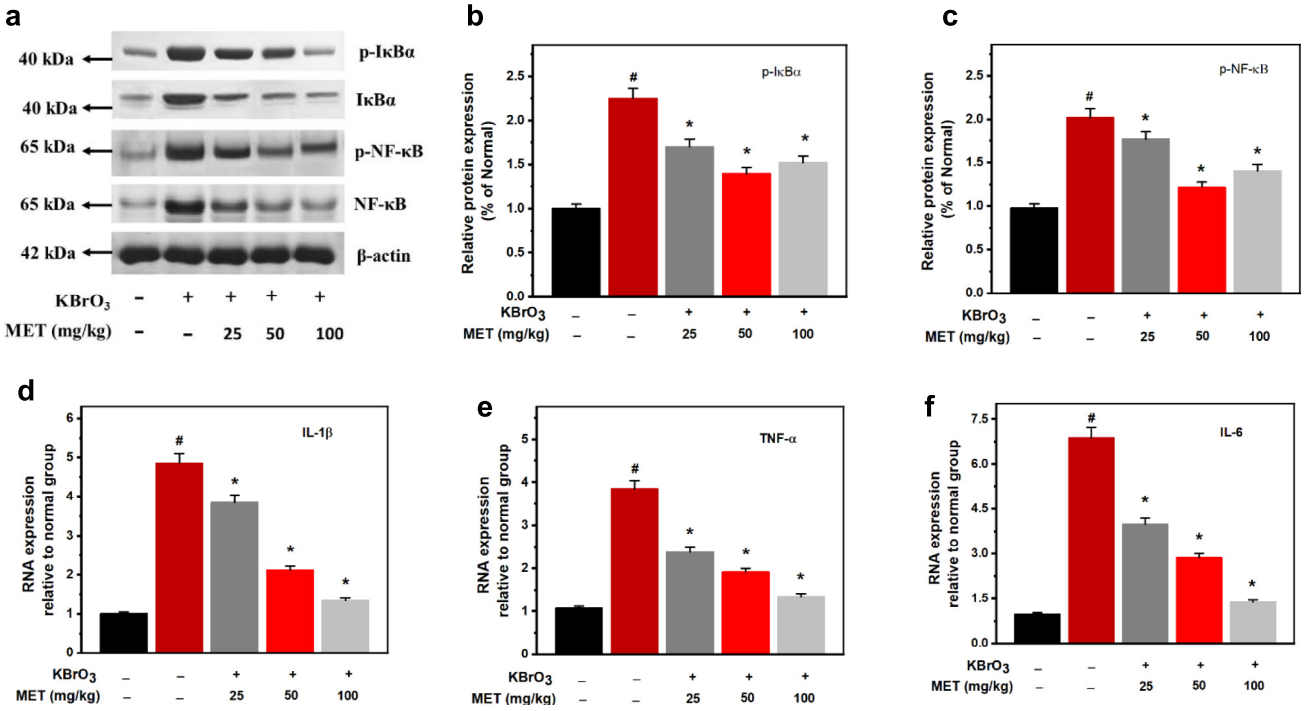

Fig. 6. Utilizing particular primary antibodies for Western blot analysis, the levels of β-actin protein served as a loading control while the expression of proteins (a-f) was examined. The mean and standard deviation of three separate investigations were assessed. #p < 0.01 vs. Normal group; *p < 0.01 vs. $KBrO_3$ group.

likely by modulating oxidative stress and enhancing endogenous antioxidant defenses. This suggests that among HepG2 cells, MET had a dominating impact towards $KBrO_3$. The amount of $KBrO_3$ can cause prominent construction of ROS in the liver which show the way to several liver-related illnesses and the potential to expand hepatocarcinoma [31]. Our findings clearly indicate that $KBrO_3$ initiates significant oxidative stress by triggering ROS production, leading to hepatic damage and apoptosis. The excessive

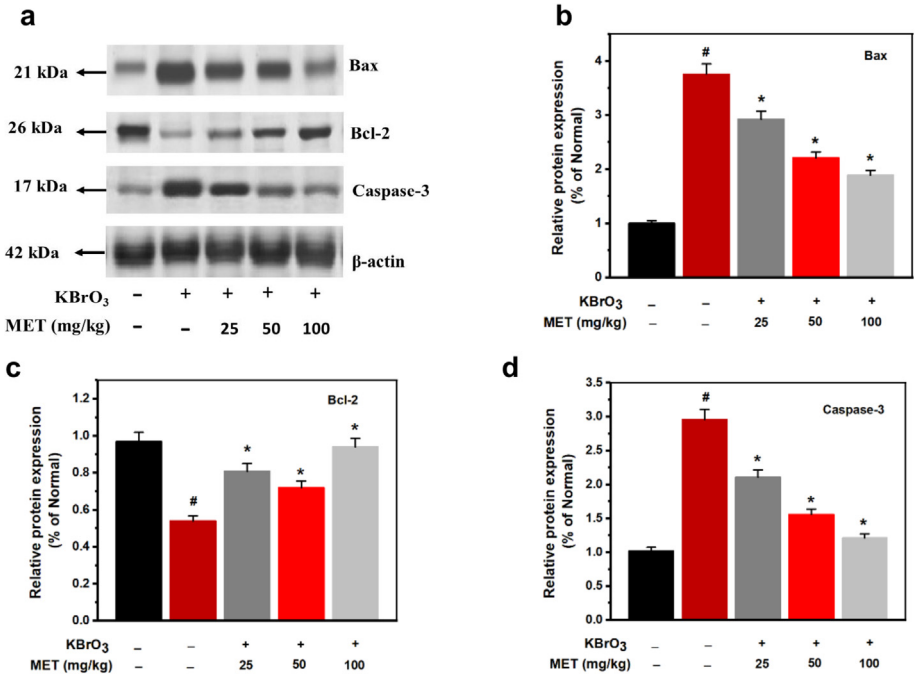

Fig. 7. Utilizing particular primary antibodies for Western blot analysis, the levels of β-actin protein served as a loading control while the expression of proteins (a-d) was examined. Densitometric measurement was used to quantify the relative amounts of proteins. #$p < 0.01$ vs. Normal group; *$p < 0.01$ vs. $KBrO_3$ group.

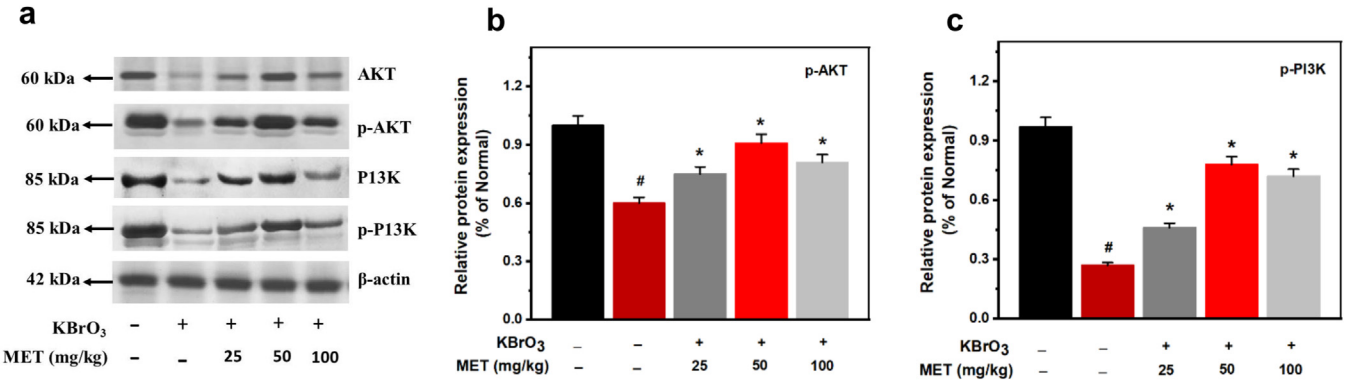

Fig. 8. The impact of MET on the signaling pathway PI3K/AKT. (a) The levels of β-actin protein served as a loading control, and the amount of expression of AKT, and PI3K was assessed. (b,c) Densitometric method was used to quantify the corresponding amounts of proteins. #$p < 0.01$ vs. Normal group; *$p < 0.01$ vs. $KBrO_3$ group.

ROS generated by $KBrO_3$ disrupts mitochondrial membrane potential, resulting in apoptotic cell death, as confirmed by previous studies [6,32]. This oxidative damage was accompanied by a marked increase in blood levels of ALT and AST, key indicators of liver injury. Histological analyses further corroborated these biochemical changes, revealing collagen deposition, disrupted lobular structure, and inflammatory cell infiltration in KBrO3-treated liver tissues.

Histological evidence further supported MET's hepatoprotective properties. MET treatment reduced collagen deposition, restored the normal lobular architecture, and diminished inflammatory cell infiltration in $KBrO_3$-exposed liver tissues. These findings parallel the work of Li et al. [24] who demonstrated MET's ability to enhance liver function and reduce histological damage in non-alcoholic fatty liver disease. Such protective effects can be attributed to MET's modulation of multiple signaling pathways, including its AMPK-dependent and independent mechanisms.

Our results also align with reports from Al-Mareed et al. [7] which showed that $KBrO_3$ exposure increases lipid peroxidation markers such as TBARS and CD while reducing antioxidant enzyme activities, including SOD and GSH. In our study, MET treatment reversed these effects, significantly lowering MDA levels and restoring SOD and GSH activities. These observations are consistent with MET's known ability to upregulate endogenous antioxidants, thereby neutralizing ROS and preventing oxidative stress. *Capparis spinosa* demonstrated its antioxidant and preventive properties towards oxidative stress and cytotoxicity caused by $KBrO_3$, according to AI-Anazi et al. [33]. In the current study, MET's antioxidant efficacy was highlighted both *in vitro* and *in vivo*. By significantly reducing ROS levels in HepG2 cells and enhancing antioxidant enzyme activities in KBrO3-exposed rats, MET effectively mitigated oxidative damage and preserved hepatic function. These results underscore the central role of ROS reduction as a mechanism through which MET protects hepatic cells from $KBrO_3$-induced toxicity. In response to $KBrO_3$ production in rats, *Sonchus asper* was observed in the current investigation regaining the levels of antioxidant enzymes like SOD, CAT, and GPx [33].

Inflammation also plays a crucial role in the pathophysiology of liver diseases. Inflammatory damage, driven by the activation of the NF-kB signaling pathway [34,35], contributes significantly to $KBrO_3$-induced liver toxicity. Once activated, NF-kB phosphorylates and degrades IkBα, releasing NF-kB subunits that induce the production of proinflammatory factors such as TNF-α, IL-6, and IL-1β [36,37]. Western blot analysis in our study demonstrated aberrant NF-kB pathway activation in the KBrO3-treated group. However, MET therapy significantly reduced the activation of NF-kB and its associated protein components, including p-IkBα/IkB. RT-PCR analysis further confirmed that MET suppressed the expression of proinflammatory cytokines, notably TNF-α, IL-6, and IL-1β, showcasing its potent anti-inflammatory effects.

In addition to addressing oxidative stress and inflammation, MET demonstrated anti-apoptotic potential. Apoptosis, a tightly regulated process controlled by caspases, Bax, and Bcl-2 family proteins, is a major consequence of $KBrO_3$-induced liver damage. Our findings revealed that MET treatment reduced the expression of pro-apoptotic markers such as Bax and caspase-3 while upregulating the anti-apoptotic protein Bcl-2. These results align with previous reports [38,39], suggesting that MET prevents apoptosis by inhibiting mitochondrial-mediated pathways and modulating caspase activity. In addition, recent studies have shown that MET can prevent apoptosis by inhibiting the mitochondrial-mediated pathway and modulating caspase activity [40]. Western blot analysis further supported MET's role in reducing apoptosis by downregulating pro-apoptotic gene expression.

Hepatocyte apoptosis and necrosis are the ultimate results of inflammation response exacerbation and amplification of several proinflammatory markers. Consequently, Western blot and RT-PCR analysis were employed to investigate the expression of relevant components in order to better understand the cellular process of MET mitigating $KBrO_3$-induced liver damage. MET's ability to modulate key signaling pathways such as NF-kB and PI3K/Akt further highlights its hepatoprotective effects. The PI3K/Akt pathway, critical in regulating cell survival, apoptosis, and inflammation, was significantly altered by KBrO3 exposure. MET treatment restored the balance by reducing Bax and caspase-3 expression and enhancing Bcl-2 levels. Western blot data indicated increased phosphorylation of PI3K and Akt in MET-treated groups, suggesting activation of this protective pathway. Additionally, MET inhibited NF-kB phosphorylation, thereby curbing the downstream inflammatory cascade.

These findings are consistent with previous studies demonstrating MET's therapeutic potential in liver diseases. Zhou et al. [41] highlighted the role of PI3K/Akt signaling in regulating cell survival and glucose metabolism, while Ding et al. [37] reported similar protective effects of natural compounds against apoptosis and inflammation in hepatocytes. Our results expand on these findings by elucidating MET's dual role in mitigating oxidative stress and inflammation while preventing apoptosis in KBrO3-induced liver damage.

5. Conclusions

Based on the aforementioned data, it was determined that metformin has a hepatoprotective impact on HepG2 cells that have been exposed to $KBrO_3$. Additionally, MET demonstrated its ability to inhibit oxidative stress and lipid peroxidation caused by $KBrO_3$. Conversely, MET raises the concentrations of antioxidants like GSH and SOD. MET treatment reverses $KBrO_3$-exposed liver injury by alleviating oxidative stress injury and NF-kB-mediated inflammatory response and apoptosis signaling pathway. In addition to serving as a guide for further investigations and therapies pertaining to liver illness, our work shows, for the initial effort, that metformin therapy may mitigate $KBrO_3$ liver toxicity.

CRediT authorship contribution statement

Bo Ma: Writing – original draft, Resources, Conceptualization. **Sheng Zheng:** Writing – original draft, Resources, Conceptualization. **Ning Xie:** Methodology. **Juan Yang:** Methodology. **Xueli Zeng:** Visualization. **Pei Liu:** Visualization. **Shunling Zhang:** Investigation. **Ji Li:** Supervision.

Ethical approval (animals)

The animal research procedures were approved by the People's Hospital of HeChuan ChongQing (Ethics approval number: 202402301) and carried out in accordance with the Guide for the Care and Use of Laboratory Animals (Ministry of Science and Technology of China, 2006).

Financial support

Basic Research Joint Special General Project of Yunnan Provincial Local Universities (part) (202301BA070001-029, 202301BA070001-044). Yunnan Province high-level scientific and technological talents and innovation team selection special – young and middle-aged academic and technical leaders reserve talent project (202405AC350067).

Declaration of competing interest

The authors declare no competing interests.

Supplementary material

https://doi.org/10.1016/j.ejbt.2025.03.002.

Data availability

Data will be made available on request.

References

[1] Vadlamani KR, Seib PA. Effect of zinc and aluminum ions in breadmaking. Cereal Chem 1999;76(3):355–60. https://doi.org/10.1094/CCHEM.1999.76.3.355.

[2] de Lahunta A, Glass E. Seizure disorders: Narcolepsy. In: de Lahunta A, Glass E, editors. Veterinary Neuroanatomy and Clinical Neurology. St Louis: Saunders Elsevier; 2009. p. 454–75. https://doi.org/10.1016/B978-0-7216-6706-5.00018-4.

[3] Nkwatoh TN, Fon TP, Navti LK. Potassium bromate in bread, health risks to bread consumers and toxicity symptoms amongst bakers in Bamenda, North West Region of Cameroon. Heliyon 2023;9(2):e13146. https://doi.org/10.1016/j.heliyon.2023.e13146. PMid: 36747561.

[4] Ahmad MK, Khan AA, Mahmood R. Taurine ameliorates potassium bromate-induced kidney damage in rats. Amino Acids 2013;45:1109–21. https://doi.org/10.1007/s00726-013-1563-4. PMid: 23913267.

[5] Oloyede OB, Sunmonu TO. Potassium bromate content of selected bread samples in Ilorin, Central Nigeria and its effect on some enzymes of rat liver and kidney. Food Chem Toxicol 2009;47(8):2067–70. https://doi.org/10.1016/j.fct.2009.05.026. PMid: 19481132.

[6] Altoom NG, Ajarem J, Allam AA, et al. Deleterious effects of potassium bromate administration on renal and hepatic tissues of Swiss mice. Saudi Journal of Biological Sciences 2018;25(2):278–84. https://doi.org/10.1016/j.sjbs.2017.01.060. PMid: 29472778.

[7] Al-Mareed AA, Farah MA, Al-Anazi KM, et al. Potassium bromate-induced oxidative stress, genotoxicity and cytotoxicity in the blood and liver cells of mice. Mutation Research/Genetic Toxicology and Environmental Mutagenesis 2022;878:503481. https://doi.org/10.1016/j.mrgentox.2022.503481. PMid: 35649675.

[8] Kujawska M, Ignatowicz E, Ewertowska M, et al. Attenuation of $KBrO_3$-induced renal and hepatic toxicity by cloudy apple juice in rat. Phytother Res 2013;27 (8):1214–9. https://doi.org/10.1002/ptr.4848. PMid: 23042583.
[9] Mohamed A, An-Naas A, Hamad H, et al. Study of histological changes in the liver and kidneys of albino mice caused by administration of potassium bromate. AlQalam J Med Appl Sci 2023;6(1):225–9. https://doi.org/10.5281/zenodo.7879051.
[10] Sabitha R, Nishi K, Gunasekaran VP, et al. p-Coumaric acid attenuates alcohol exposed hepatic injury through MAPKs, apoptosis and Nrf2 signaling in experimental models. Chem Biol Interact 2020;321:109044. https://doi.org/10.1016/j.cbi.2020.109044. PMid: 32151596.
[11] Liang WF, Gong YX, Li HF, et al. Curcumin activates ROS signaling to promote pyroptosis in hepatocellular carcinoma HepG2 cells. In Vivo 2021;35 (1):249–57. https://doi.org/10.21873/invivo.12253. PMid: 33402471.
[12] Li S, Hong M, Tan HY, et al. Insights into the role and interdependence of oxidative stress and inflammation in liver diseases. Oxid Med Cell Longev 2016;2016(1):4234061. https://doi.org/10.1155/2016/4234061. PMid: 28070230.
[13] Rajendran P, Ammar RB, Al-Saeedi FJ, et al. Kaempferol inhibits zearalenone-induced oxidative stress and apoptosis via the PI3K/Akt-mediated Nrf2 signaling pathway: *In vitro* and *in vivo* studies. Int J Mol Sci 2020;22(1):217. https://doi.org/10.3390/ijms22010217. PMid: 33379332.
[14] Ben Ammar R, Abdulaziz Alamer S, Elsayed Mohamed M, et al. Potential inhibitory effect of geraniol isolated from lemongrass (*Cymbopogon commutatus* Stapf) on tilmicosin-induced oxidative stress in cardiac tissue. Nat Prod Res 2023;38(10):1652–61. https://doi.org/10.1080/14786419.2023.2215901. PMid: 37226502.
[15] Rajendran P, Renu K, Abdallah BM, et al. Nimbolide: Promising agent for prevention and treatment of chronic diseases (recent update). Food Nutr Res 2024;68:9650. https://doi.org/10.29219/fnr.v68.9650. PMid: 38571915.
[16] Liu W, Wang Z, Hou JG, et al. The liver protection effects of maltol, a flavoring agent, on carbon tetrachloride-induced acute liver injury in mice via inhibiting apoptosis and inflammatory response. Molecules 2018;23(9):2120. https://doi.org/10.3390/molecules23092120. PMid: 30142916.
[17] Cui Y, Jiang L, Shao Y, et al. Anti-alcohol liver disease effect of *Gentianae macrophyllae* extract through MAPK/JNK/p38 pathway. J Pharm Pharmacol 2019;71(2):240–50. https://doi.org/10.1111/jphp.13027. PMid: 30298517.
[18] Wang D, Gao Q, Wang T, et al. Green tea infusion protects against alcoholic liver injury by attenuating inflammation and regulating the PI3K/Akt/eNOS pathway in C57BL/6 mice. Food Funct 2017;8(9):3165–77. https://doi.org/10.1039/C7FO00791D. PMid: 28782772.
[19] Foretz M, Guigas B, Viollet B. Metformin: Update on mechanisms of action and repurposing potential. Nat Rev Endocrinol 2023;19:460–76. https://doi.org/10.1038/s41574-023-00833-4. PMid: 37130947.
[20] Madiraju AK, Erion DM, Rahimi Y, et al. Metformin suppresses gluconeogenesis by inhibiting mitochondrial glycerophosphate dehydrogenase. Nature 2014;510(7506):542–6. https://doi.org/10.1038/nature13270. PMid: 24847880.
[21] Xu H, Zhou Y, Liu Y, et al. Metformin improves hepatic IRS2/PI3K/Akt signaling in insulin-resistant rats of NASH and cirrhosis. J Endocrinol 2016;229 (2):133–44. https://doi.org/10.1530/JOE-15-0409 PMid:26941037.
[22] Bhat A, Sebastiani G, Bhat M. Systematic review: Preventive and therapeutic applications of metformin in liver disease. World J Hepatol 2015;7 (12):1652–9. https://doi.org/10.4254/wjh.v7.i12.1652. PMid: 26140084.
[23] Khezri MR, Varzandeh R, Ghasemnejad-Berenji M. Protective effects of metformin against aluminum phosphide-induced acute hepato-renal damage in rats: An experimental approach. Pestic Biochem Physiol 2022;188:105258. https://doi.org/10.1016/j.pestbp.2022.105258. PMid: 36464363.
[24] Li X, Wang L, Yang X, et al. Metformin attenuates ischemia-reperfusion injury of fatty liver in rats through inhibition of the TLR4/NF-κB axis. Balkan Med J 2020;37(4):196–202. https://doi.org/10.4274/balkanmedj.galenos.2020.2019.9.31. PMid: 32270948.
[25] Cao L, Zhi D, Han J, et al. Combinational effect of curcumin and metformin against gentamicin-induced nephrotoxicity: Involvement of antioxidative, anti-inflammatory and antiapoptotic pathway. J Food Biochem 2019;43(7): e12836. https://doi.org/10.1111/jfbc.12836. PMid: 31353717.
[26] Nivetha S, Asha KRT, Srinivasan S, et al. Hepatoprotective effect of p-Coumaric acid against $KBrO_3$-induced apoptosis in HepG2 cells. Cell Biochem Funct 2023;41(7):868–75. https://doi.org/10.1002/cbf.3837. PMid: 37573567.
[27] Peng M, Darko KO, Tao T, et al. Combination of metformin with chemotherapeutic drugs via different molecular mechanisms. Cancer Treat Rev 2017;54:24–33. https://doi.org/10.1016/j.ctrv.2017.01.005. PMid: 28161619.
[28] LaMoia TE, Shulman GS. Cellular and molecular mechanisms of metformin action. Endocr Rev 2021;42(1):77–96. https://doi.org/10.1210/endrev/bnaa023. PMid: 32897388.
[29] Lv Z, Guo Y. Metformin and its benefits for various diseases. Front Endocrinol 2020;11:191. https://doi.org/10.3389/fendo.2020.00191. PMid: 32425881.
[30] Cahova M, Palenickova E, Dankova H, et al. Metformin prevents ischemia reperfusion-induced oxidative stress in the fatty liver by attenuation of reactive oxygen species formation. Am J Physiol-Gastrointest Liver Physiol 2015;309(2):G100–11. https://doi.org/10.1152/ajpgi.00329.2014.
[31] Xu J, Zhang G, Tong Y, et al. Corilagin induces apoptosis, autophagy and ROS generation in gastric cancer cells *in vitro*. Int J Mol Med 2019;43(2):967–79. https://doi.org/10.3892/ijmm.2018.4031. PMid: 30569134.
[32] Ahmad MK, Khan AA, Ali SN, et al. Chemoprotective effect of taurine on potassium bromate-induced DNA damage, DNA-protein cross-linking and oxidative stress in rat intestine. PLoS One 2015;10(3):e0119137. https://doi.org/10.1371/journal.pone.0119137. PMid: 25748174.
[33] Al-Anazi KM, Al-Mareed AA, Farah MA, et al. Protective effect of *Capparis spinosa* extract against potassium bromate induced oxidative stress and genotoxicity in mice. Evid Based Complement Alternat Med 2021;2021:8875238. https://doi.org/10.1155/2021/8875238. PMid: 33531925.
[34] Balkwill F, Charles KA, Mantovani A. Smoldering and polarized inflammation in the initiation and promotion of malignant disease. Cancer Cell 2005;7 (3):211–7. https://doi.org/10.1016/j.ccr.2005.02.013. PMid: 15766659.
[35] Fan H, Tu T, Zhang X, et al. Sinomenine attenuates alcohol-induced acute liver injury via inhibiting oxidative stress, inflammation and apoptosis in mice. Food Chem Toxicol 2022;159:112759. https://doi.org/10.1016/j.fct.2021.112759. PMid: 34883223.
[36] Cildir G, Low KC, Tergaonkar V. Noncanonical NF-κB signaling in health and disease. Trends Mol Med 2016;22(5):414–29. https://doi.org/10.1016/j.molmed.2016.03.002. PMid: 27068135.
[37] Ding C, Zhao Y, Chen X, et al. Taxifolin, a novel food, attenuates acute alcohol-induced liver injury in mice through regulating the NF-κB-mediated inflammation and PI3K/Akt signalling pathways. Pharm Biol 2021;59 (1):866–77. https://doi.org/10.1080/13880209.2021.1942504. PMid: 34225578.
[38] Czabotar PE, Lessene G, Strasser A, et al. Control of apoptosis by the BCL-2 protein family: Implications for physiology and therapy. Nat Rev Mol Cell Biol 2014;15(1):49–63. https://doi.org/10.1038/nrm3722. PMid: 24355989.
[39] Agrawal SN. The vital phenomena of apoptosis: A review. South Asian Res J Med Sci 2019;1(1):15–9. https://doi.org/10.36346/sarjms.2019.v01i01.004.
[40] Mohamed EK, Hafez DM. Gallic acid and metformin co-administration reduce oxidative stress, apoptosis and inflammation via Fas/caspase-3 and NF-κB signaling pathways in thioacetamide-induced acute hepatic encephalopathy in rats. BMC Complementary Med Ther 2023;23(1):265. https://doi.org/10.1186/s12906-023-04067-9. PMid: 37491245.
[41] Zhou YD, Hou JG, Liu W, et al. 20(*R*)-ginsenoside Rg3, a rare saponin from red ginseng, ameliorates acetaminophen-induced hepatotoxicity by suppressing PI3K/AKT pathway-mediated inflammation and apoptosis. Int Immunopharmacol 2018;59:21–30. https://doi.org/10.1016/j.intimp.2018.03.030. PMid: 29621733.